Constructing Symbolic Models for the Input/Output Behavior of Periodically Time-Varying Systems Using Harmonic Transfer Matrices

Piet Vanassche, Georges Gielen and Willy Sansen
Katholieke Universiteit Leuven, Department of Electrical Engineering, ESAT-MICAS
Kasteelpark Arenberg 10, B-3001 Leuven, Belgium

Abstract

A new technique is presented for generating symbolic expressions for the harmonic transfer functions of linear periodically time-varying (LPTV) systems, like mixers and PLL's. The algorithm, which we call Symbolic HTM, is based on the organisation of the harmonic transfer functions into a harmonic transfer matrix. This representation allows to manipulate LPTV systems in a way that is similar to linear time-invariant (LTI) systems, making it possible to generate symbolic expressions which relate the overall harmonic transfer functions to the characteristics of the building blocks. These expressions can be used as design equations or as parametrized models for use in simulations. The algorithm is illustrated for a downconversion mixer.

1 Introduction

Symbolic expressions relating the behavior of a system or circuit to it's building block characteristics are useful for several reasons [3]. First of all, they offer the designer explicit relations that provide insight into the system's overall behavior and characteristics. They can also be used to make decisions about building block and component parameters. Finally, they provide parametrized, behavioral models which can be used in simulations at higher levels of abstraction. The fact that these models are symbolic avoids the necessity to recompute them each time a new set of parameter values is introduced, which is for example useful in perfoming trade-off analyses. Up to now, most of the research on symbolic analysis has been restricted to linear (small-signal) circuit characteristics [2], with some extensions to weakly nonlinear circuits [12], [13].

This paper presents an algorithm to construct symbolic expressions for the harmonic transfer functions $H_i(s)$ of linear periodically time-varying (LPTV) systems, like mixers and PLL's. These harmonic transfer functions are defined in Fig. 1, which shows a generic model for the input/output behavior of an LPTV system. As can be seen, there are several paths from input to output, each path consisting of a linear time-invariant (LTI) filter $H_i(s)$ and a frequency translation. The frequency translations result in the fact that (undesired) signal components from anywhere in the input spectrum get converted into the wanted output signal band. The filters $H_i(s)$ determine the "strength" of this signal transfer between the different frequency bands and, for this reason, are called the harmonic transfer functions. Knowing the $H_i(s)$ provides us with a frequency-domain characterization of the LPTV system behavior, helping for example in estimating the impact of sideband signal components in mixing applications and that of noise sources on the output spectrum of a PLL.

Using harmonic transfer functions to analyse time-varying behavior occurs in many areas of electrical engineering. As electronic circuits are concerned, an algorithm to compute them numerically, starting from a netlist, is presented in [10]. Although this approach is very well suited for verification and the construction of numerical macromodels, it does not offer clear insight into the system's

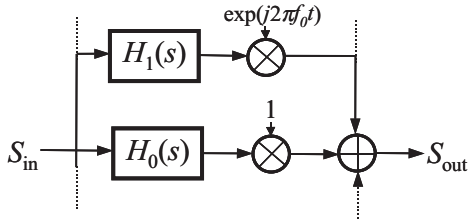

Figure 1. Generic model of an LPTV system. Each input-output path consists of an LTI filtering stage followed by a frequency translation.

internal structure and it's dependencies upon building block characteristics. In [8] (and also in [9]), it is proposed to organize the harmonic transfer functions into a single harmonic transfer matrix (HTM). This allows to manipulate time-varying systems in a way similar to (multi-variable) LTI systems. Although offering better insights into the system's internal structure, the approach in [8] is still made from a numerical point of view, requiring numerical values for all design parameters.

At this point it is worth emphasizing that LPTV systems are inherently *linear*. Although one would be tempted to consider the multiplications with $e^{jk\omega_0 t}$ in Fig. 1 as nonlinear, the principle of superposition still holds, making them linear operations. Symbolic computation of the harmonic transfer functions using techniques for nonlinear symbolic LTI network analysis [12], [13] will hence not fully exploit the linear nature of LPTV systems. This makes them suboptimal for this kind of applications.

In our work, the organisation of harmonic transfer functions into harmonic transfer matrices is used and extended as a framework for symbolic manipulation of LPTV systems. The method is called Symbolic HTM. The input is a system model in the form of a block diagram. The output consists of symbolic expressions for the system's harmonic transfer functions. The required input models can be extracted from netlists with the help of existing tools for behavioral modeling [6]. Hereby, large LTI subcircuits can be represented using their multiport parameters. With Symbolic HTM expressing results in terms of these multiport parameters, lengthy and uninterpretable expressions are avoided. Computation of the multiport parameter characteristics can then be done afterwards, using well-established techniques for (LTI) symbolic circuit analysis [2], [4], [7]. In the hierarchy of symbolic analysis, this work hence makes up a layer on top of the existing tools for symbolic network analysis.

The remainder of the paper is organized as follows. In section 2, we recapitulate the essentials about harmonic transfer functions of LPTV systems and introduce their organization into harmonic transfer matrices. In section 3, we show how this representation can be used for efficient manipulation of LPTV systems. An algorithm for symbolic computation of the overall input/output behavior is described in section 4. Section 5 presents the results obtained

from the analysis of a downconversion mixer and finally, conclusions are drawn in section 6.

2 Harmonic transfer matrix system representation

Considering a general linear time-varying system, it's input-output relation is described by [15],

$$y(t) = \int_{-\infty}^{+\infty} h(t,r)u(r)dr \tag{1}$$

where $u(t)$ represents the input and $y(t)$ the output signal(s) (for notational convenience, we denote $u(t)$ and $y(t)$ as scalars; they can however also be considered as vectors in which case $h(t,r)$ becomes a matrix). For a T-periodic (LPTV) system, $h(t,r)$ will be periodic with respect to displacements in both of it's arguments, or

$$h(t+T, r+T) = h(t,r) \;\; \forall t, r \in \Re \tag{2}$$

Changing variables to $r = t - \tau$, we can write (1) as

$$y(t) = \int_{-\infty}^{+\infty} h(t, t-\tau)u(t-\tau)d\tau \tag{3}$$

where it is easily seen that $h(t, t-\tau)$ is T-periodic in t. The latter implies that

$$h(t, t-\tau) = \sum_{k=-\infty}^{k=+\infty} h_k(\tau)e^{jk\omega_0 t} \tag{4}$$

with $\omega_0 = 2\pi f_0 = 2\pi/T$ and

$$h_k(\tau) = \frac{1}{T}\int_0^T h(t, t-\tau)e^{-jk\omega_0 t}dt \tag{5}$$

Substituting equation (4) into equation (3) finally yields

$$y(t) = \sum_{k=-\infty}^{k=+\infty} e^{jk\omega_0 t}\int_{-\infty}^{+\infty} h_k(\tau)u(t-\tau) \tag{6}$$

Analyzing expression (6), we see that the output signal $y(t)$ consists of a set of terms that are frequency translated (factor $e^{jk\omega_0 t}$), LTI filtered (factor $\int_{-\infty}^{+\infty} h_k(\tau)u(t-\tau)d\tau$) transformations of the input signal $u(t)$. This corresponds to the model as pictured in Fig. 1. The functions $h_k(t)$ are referred to as the harmonic impulse responses, while their Laplace transforms

$$H_k(s) = \int_{-\infty}^{+\infty} h_k(\tau)e^{-s\tau}d\tau \tag{7}$$

are called the harmonic transfer functions (HTF). These transfer functions completely characterize the (linear part of) the behavior of a periodic system.

Using the HTF's, we can convert the time-domain input/output relation (6) to the Laplace domain, or

$$Y(s) = \sum_{k=-\infty}^{k=+\infty} H_k(s - jk\omega_0)U(s - jk\omega_0) \tag{8}$$

with $U(s)$ and $Y(s)$ the Laplace transforms of respectively $u(t)$ and $y(t)$. In [8] (and also in [9]), it was observed that with proper organization of the datastructures, the input/output relation (7) can be rewritten in a way that resembles the description of ordinary LTI systems. Introducing

$$\tilde{\mathbf{U}}(s) = \begin{bmatrix} \ldots & \tilde{U}_{-1}(s) & \tilde{U}_0(s) & \tilde{U}_1(s) & \ldots \end{bmatrix}^T \tag{9}$$

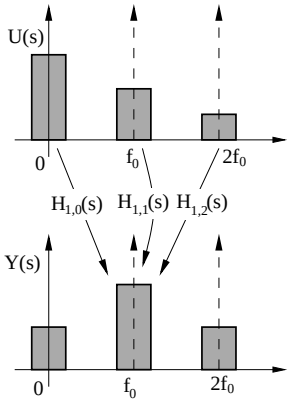

Figure 2. Signal transfers between the different input frequency bands and output frequency bands.

with $\tilde{U}_k(s) = U(s + jk\omega_0)$ and with a similar definition for $\tilde{\mathbf{Y}}(s)$, (8) can be written as

$$\tilde{\mathbf{Y}}(s) = \tilde{\mathbf{H}}(s)\tilde{\mathbf{U}}(s) \tag{10}$$

with $\tilde{\mathbf{H}}(s)$ the doubly infinite matrix

$$\tilde{\mathbf{H}}(s) = \begin{bmatrix} \vdots & \vdots & \vdots & \\ \cdots & \tilde{H}_{-1,-1}(s) & \tilde{H}_{-1,0}(s) & \tilde{H}_{-1,1}(s) & \cdots \\ \cdots & \tilde{H}_{0,-1}(s) & \tilde{H}_{0,0}(s) & \tilde{H}_{0,1}(s) & \cdots \\ \cdots & \tilde{H}_{1,-1}(s) & \tilde{H}_{1,0}(s) & \tilde{H}_{1,1}(s) & \cdots \\ & \vdots & \vdots & \vdots & \end{bmatrix} \tag{11}$$

where

$$\tilde{H}_{n,m}(s) = H_{n-m}(s + jm\omega_0) \tag{12}$$

This matrix $\tilde{\mathbf{H}}(s)$ is called the *harmonic transfer matrix* (HTM) of the LPTV system. The tilde on top of it's name is used to distinguish it from an ordinary LTI multivariable system matrix.

The nature of the HTM elements $\tilde{H}_{n,m}(s)$ follows from the observation that the vector component $\tilde{U}_m(s) = U(s + jm\omega_0)$ models the signal content in the frequency band centered around $m\omega_0$. This, together with the input/output relation

$$\tilde{Y}_n(s) = \sum_m \tilde{H}_{n,m}(s)\tilde{U}_m(s) \tag{13}$$

makes clear that the HTM element $\tilde{H}_{n,m}(s)$ models the transfer of signal content from the input signal frequency band around $m\omega_0$ to the output signal frequency band around $n\omega_0$. These transfers and their relation to the HTM elements $\tilde{H}_{n,m}(s)$ are illustrated in Fig. 2.

3 LPTV system manipulation using HTM's

HTM's provide us with an efficient framework to manipulate LPTV systems and to compute the overall input/output behavior given the system's building block characteristics. To this account, section 3.1 introduces the HTM's of some elementary systems. The basic apparatus for computing the HTM's of composed systems is outlined in section 3.2. Special focus is given to the fact that the results should be symbolically applicable.

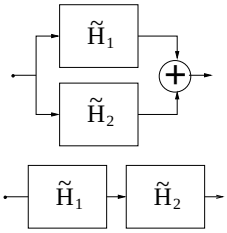

Figure 3. Parallel and series connection of two (LPTV) systems.

3.1 HTM's of elementary systems

Two fundamental subclasses of LPTV systems are LTI systems on the one hand and multiplications with a known periodic reference signal $p(t)$ on the other hand. Any other LPTV system can always be modeled as an interconnection of these basic subclasses. Finding the HTM's for these special type of LPTV systems is straightforward.

Considering the input/output relation (6), it holds, by definition, that for an LTI system $h_k(\tau) = 0$ except for $k = 0$. The HTM of an LTI operator with transfer characteristic $H(s)$ is hence given by

$$\begin{cases} \tilde{H}_{n,m}(s) &= H(s + jm\omega_0) & m = n \\ \tilde{H}_{n,m}(s) &= 0 & m \neq n \end{cases} \tag{14}$$

This implies that the HTM equivalent of an LTI system is a diagonal matrix with it's frequency-shifted transfer characteristic on the diagonal.

The HTM of a multiplication of the input signal $u(t)$ with a T-periodic signal $p(t)$, or $y(t) = p(t)u(t)$, where

$$p(t) = \sum_k P_k e^{jk\omega_0 t} \tag{15}$$

can be found by observing that this corresponds with $h_k(\tau) = P_k\delta(\tau)$ with $\delta(\tau)$ being a Dirac impulse. The HTM elements then become $\tilde{H}_{n,m} = P_{n-m}$, or

$$\tilde{\mathbf{H}}(s) = \begin{bmatrix} \ddots & \ddots & \ddots & & \\ & P_0 & P_{-1} & P_{-2} & \\ \ddots & P_1 & P_0 & P_{-1} & \ddots \\ & P_2 & P_1 & P_0 & \\ & & \ddots & \ddots & \ddots \end{bmatrix} \tag{16}$$

which is a frequency-independent Toeplitz matrix.

3.2 HTM's of composed systems

In constructing and manipulating linear systems, there are three types of basic connections, being parallel, series and feedback connections. Together, they make up a complete set which can be used to construct block diagrams or any other type of graph.

Given the HTM's $\tilde{\mathbf{H}}_1(s)$ and $\tilde{\mathbf{H}}_2(s)$ of two LPTV systems, it is easy to show that the HTM of their parallel respectively series connection, as illustrated in Fig. 3, is given by

$$\tilde{\mathbf{H}}_+(s) = \tilde{\mathbf{H}}_1(s) + \tilde{\mathbf{H}}_2(s) \tag{17}$$

$$\tilde{\mathbf{H}}_\times(s) = \tilde{\mathbf{H}}_2(s)\tilde{\mathbf{H}}_1(s) \tag{18}$$

It is important to note that the order of multiplication in (18) cannot be interchanged. Contrary to single-input single-output LTI systems, LPTV systems are, in general, not commutable.

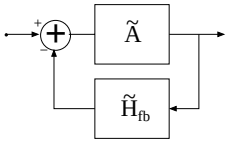

Figure 4. Feedback connection of two (LPTV) systems.

As the HTM of the feedback connection in Fig. 4 is concerned, things are more involved. Straightforward manipulation yields for the closed loop characteristic $\tilde{\mathbf{H}}_{cl}(s)$

$$\tilde{\mathbf{H}}_{cl}(s) = \left(\mathbf{I} + \tilde{\mathbf{G}}(\mathbf{s})\right)^{-1} \tilde{\mathbf{A}}(s) \tag{19}$$

with $\tilde{\mathbf{G}}(s) = \tilde{\mathbf{A}}(s)\tilde{\mathbf{H}}_{fb}(s)$ the open loop gain HTM and $\mathbf{I}$ the identity matrix. Computing $\tilde{\mathbf{H}}_{cl}(s)$ hence involves a matrix inversion which is a hard problem to solve symbolically. However, in most practical LPTV systems, the HTM's that need to be inverted ($\mathbf{I} + \tilde{\mathbf{G}}(\mathbf{s})$ in case of the feedback example) tend to have a dominant diagonal component, meaning that the energy contained in the diagonal elements is much larger than the energy contained in the sideband elements. This corresponds to a dominant LTI component being present in the overall LPTV feedback path. From a control theory point of view, the presence of this dominant diagonal component can be explained by the fact that feedback systems (which generate the need for HTM inversions) without such a dominant diagonal component will tend to be rather unstable.

Assuming the presence of a dominant diagonal component, the inversion of a HTM $\tilde{\mathbf{H}}(s)$ can be approximated using a series expansion, that can easily be evaluated symbolically. Writing $\tilde{\mathbf{H}}(s) = \tilde{\mathbf{D}}(s) - \tilde{\mathbf{F}}(s)$, where $\tilde{\mathbf{D}}(s)$ contains the diagonal elements of $\tilde{\mathbf{H}}(s)$ and $-\tilde{\mathbf{F}}(s)$ the off-diagonal elements, inversion yields

$$\tilde{\mathbf{H}}(s)^{-1} = \left(\mathbf{I} - \tilde{\mathbf{D}}(\mathbf{s})^{-\mathbf{1}}\tilde{\mathbf{F}}(\mathbf{s})\right)^{-1} \tilde{\mathbf{D}}(s)^{-1} \tag{20}$$

$$= \sum_{r=0}^{\infty} \left(\tilde{\mathbf{D}}(s)^{-1}\tilde{\mathbf{F}}(s)\right)^r \tilde{\mathbf{D}}(s)^{-1} \tag{21}$$

The expansion (21) is convergent as long as $\left\|\tilde{\mathbf{D}}(s)^{-1}\tilde{\mathbf{F}}(s)\right\| < 1$ [5]. For practical purposes, it will be truncated after a finite number of terms R. This R can be user-provided or can be based upon error estimations if numerical data is available. As a final note, we mention that if the expansion (21) is not applicable ($\left\|\tilde{\mathbf{D}}(s)^{-1}\tilde{\mathbf{F}}(s)\right\| > 1$), other techniques, like determinant expansion techniques as applied in classical symbolic circuit analysis [4], need to be tried for computation of the inverse.

4 Computing the input/output HTM

In what follows the HTM framework is used as a foundation for the Symbolic HTM algorithm, generating symbolic expressions for the overall input/output HTFs. The algorithm takes a block diagram as input. The composing blocks can be LTI systems, represented by a symbol $H(s)$ for the transfer characteristic, multiplications with a periodic signal $p(t)$, represented by the symbols P_k for the Fourier coefficients of $p(t)$, or even other LPTV systems, represented by the symbols $H_k(s)$ for the HTFs. Expressions are generated in terms of the symbols representing the building blocks. This allows for a hierarchical approach, where for example the detailed characteristics of LTI subsystems are extracted afterwards using standard techniques for symbolic LTI network analysis [2], [4], [7].

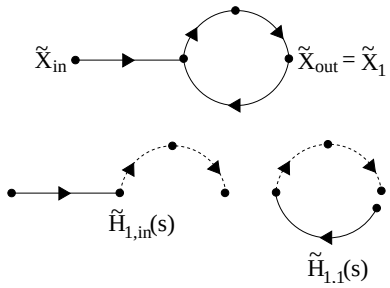

Figure 5. Graphs representing a feedback system (top) and it's open loop HTM's (bottom).

In the next couple of sections, we discuss both the symbolic HTM datastructures (section 4.1) and its computational flow (section 4.2).

4.1 Datastructures

In storing the HTM, it is not needed to store every matrix element separately. Looking at the element definitions in (12), it is observed that the HTM has a semi-Toeplitz structure in a sense that a diagonal for which $n - m = k$ contains frequency shifted copies of the same HTF $H_k(s)$. It is therfore sufficient to only store the (nonzero) HTFs in order to be able to compute all necessary elements of the harmonic transfer matrix.

4.2 Computational flow

Symbolic HTM's computational flow consists of three steps. In a first (preprocessing) step, the input model feedback loops are cut by introducing a set of loop variables. During the second step, which comprises the actual symbolic computations, these loop variables are eliminated in order to obtain symbolic expressions for the input/output HTFs. In a final (postprocessing) step, these expressions can be simplified if numerical data is available.

Breaking the loops: In a first step, all loops are cut. This results in the introduction of a set of loop variables. Given a graph-like representation, loops can be detected using graph traversal algorithms [11]. They are cut at the point where they first leave the feedforward path. This process results in a set of equations

$$\begin{cases} \tilde{\mathbf{X}}_1(s) &= \sum \tilde{\mathbf{H}}_{1,k}(s)\tilde{\mathbf{X}}_k(s) + \tilde{\mathbf{H}}_{1,in}\tilde{\mathbf{U}}(s) \\ \tilde{\mathbf{X}}_2(s) &= \sum \tilde{\mathbf{H}}_{2,k}(s)\tilde{\mathbf{X}}_k(s) + \tilde{\mathbf{H}}_{2,in}\tilde{\mathbf{U}}(s) \\ &\vdots \\ \tilde{\mathbf{Y}}(s) &= \sum \tilde{\mathbf{H}}_{y,k}(s)\tilde{\mathbf{X}}_k(s) + \tilde{\mathbf{H}}_{y,in}\tilde{\mathbf{U}}(s) \end{cases} \tag{22}$$

with the $\tilde{\mathbf{X}}_k(s)$ representing the loop variables (with a structure as defined by (9)) and the $\tilde{\mathbf{H}}_{l,\cdot}(s)$, $l = 1, 2, \ldots$, being the HTM's characterizing the open loop behavior. These open loop HTM's are computed as series and/or parallel connections of the building block HTM's, using the principles outlined in section 3.2. As a heuristic for obtaining better readable expressions, for each loop equation l, a symbolic name can be assigned to the HTM corresponding to the intersection of the graphs of the open loop HTM's $\tilde{\mathbf{H}}_{l,\cdot}(s)$. This means that one introduces auxiliary symbols to represent the HTM corresponding to the part in common to the $\tilde{\mathbf{H}}_{l,\cdot}(s)$. Expressing the $\tilde{\mathbf{H}}_{l,\cdot}(s)$ in terms of these auxiliary symbols, yields hierarchically structured and better readable expressions.

All of this is illustrated in Fig. 5 for the case of a simple feedback system. The top graph represents the graph of the overall system. Each branch represents a (possibly time-varying) building block. There is one feedback loop leading to the introduction of a loop variable $\tilde{\mathbf{X}}_1$ and it's corresponding loop equation. The bottom part of Fig. 5 shows the graphs corresponding to the open loop HTM's $\tilde{\mathbf{H}}_{1,\cdot}(s)$. Here, the dashed part is in common to both graphs and it's corresponding HTM could be represented using auxilary symbols in order to make further expressions better readable.

Eliminating the loop variables: In a second step, the loop variables $\tilde{\mathbf{X}}_k(s)$ are eliminated using symbolic Gaussian elimination. For $\tilde{\mathbf{X}}_1(s)$, this implies that we solve

$$\left(\mathbf{I} - \tilde{\mathbf{H}}_{\mathbf{11}}(\mathbf{s})\right) \tilde{\mathbf{X}}_1(s) = \sum_{k>1} \tilde{\mathbf{H}}_{1,k}(s)\tilde{\mathbf{X}}_k(s) + \tilde{\mathbf{H}}_{1,in}\tilde{\mathbf{U}}(s) \tag{23}$$

and substitute the result into the equations for $\tilde{\mathbf{X}}_2(s), \tilde{\mathbf{X}}_3(s), \ldots$ in (22). The result is a reduced system with one equation and one variable removed. We proceed in a likewise manner to eliminate the other loop variables until we end up with the desired input/output relation.

The inversion of $\left(\mathbf{I} - \tilde{\mathbf{H}}_{\mathbf{11}}(\mathbf{s})\right)$, implied in equation (23), is performed using the series expansion (21) truncated after the first R terms. R should be provided by the user, unless numerical data is available, allowing to determine it's value based upon error control.

During computations, a number of simple measures can be taken to avoid wasting time on unimportant contributions. Firstly, we can limit the number of tones, i.e. the number of HTF's being stored and computed. This implies that for each LPTV subsystem and interconnection of subsystems, we assume that the HTF's $H_k(s) = 0$ for $|k| > K$, skipping their exact computation. Secondly, in performing the inversions, we introduce a dummy variable μ in the expansion (21), writing

$$\tilde{\mathbf{H}}(s)^{-1} \approx \sum_{r=0}^{R-1} \mu^r \left(\tilde{\mathbf{D}}(s)^{-1}\tilde{\mathbf{F}}(s)\right)^r \tilde{\mathbf{D}}(s)^{-1} \tag{24}$$

This dummy variable μ is carried along during all inversion and substitution processes. As a heuristic for computing only the relevant terms, it is assumed that all contributions which are $O\left(\mu^R\right)$ are unimportant and hence can be neglected.

Simplification: In a final step, the computed expressions can be simplified by eliminating all terms with neglegible energy. This is however only possible if numerical data is available to control the simplification error [2], [14].

Computational complexity: The complexity of this algorithm is roughly proportional to the total number of all terms generated during the second (elimination) step. This number is (in worst case) of the order $O\left(N\left(2K+1\right)^{R+N-1} T^{R+N-1}\right)$, where N is the number of time-varying feedback loops, K is a measure for the number of tones taken into account (as defined above), T is the average number of terms necessary for modeling the open loop HTM elements and $R-1$ is the order in μ up to which the contributions are computed.

5 Experimental results

The Symbolic HTM algorithm has been prototyped in Maple. It was applied to the linear downconversion mixer shown in Fig. 6. For the given application, the algorithm takes a few seconds to execute on a Sun ULTRA 30. In what follows, the mixer building

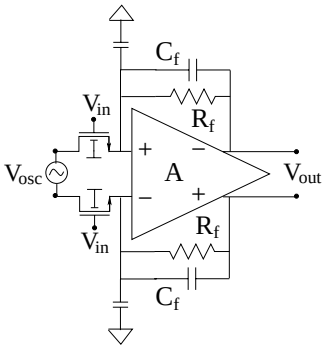

Figure 6. The linear down conversion mixer.

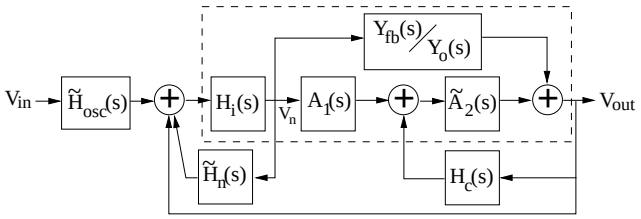

Figure 7. Block diagram of the linear downconversion mixer. A tilde on top of the name indicates that the block is time-varying.

block models are discussed, some remarks concerning the construction of the loop equations (22) are made and the resulting symbolic expressions are verified against numerical computations.

The mixer behavior was modeled assuming the amplifier to be a two-stage Miller-OTA. Both OTA stages were represented by their (time-varying) Y-parameter equivalents. The mixer block diagram shown in Fig. 7 was then extracted from the (linearized) nodal equations of the circuit in Fig. 6. The time-varying subblocks are indicated by a tilde on top of their name. The main sources of time-varying behavior are due to the modulation of the small-signal parameters of the input transistors as well as those of the second OTA stage. The input transistor models are based upon the level-1 equations for a MOST in triode region. This yields the small-signal current model

$$i_{DS} = \beta V_{osc}(t) v_G - \beta \left(V_G - V_T\right) v_n - \gamma \beta V_n(t) v_n \qquad (25)$$

where we use capital letters to represent the (time-varying) operating points and small letters for the small-signal values. Here, $V_{osc}(t)$ is the oscillator signal, $V_n(t)$ is the signal at the OTA input terminals and γ is a factor modeling the mismatch between the two input transistors. The first term in equation (25) represents the desired mixing behavior, while the last term adds a time-varying component to the OTA input admittance. The second time-varying contribution, due to the 3rd order nonlinear behavior of the transconductance of the second OTA stage, involves the modulated small-signal transconductance

$$g_{m2}(t) = \sum_k g_{m2,k} e^{jk\omega_0 t} \qquad (26)$$

As a first step of the symbolic HTM algorithm, the loop equations (22) were constructed. During this process, two loop variables and one auxilary HTM, which we call $\tilde{\mathbf{G}}(s)$, were introduced. This auxilary HTM corresponds to to the part encircled by the dashed line in Fig. 7, and was generated as the intersection of the graphs corresponding to the open loop HTMs of the second loop equation. It represents a system with HTFs

$$\begin{cases} G_0(s) &= \frac{H_i(s)\left(A_1(s)\left(g_{m2,0}+sC_c\right)+Y_{fb}(s)\right)}{Y_o(s)} \\ G_k(s) &= \frac{H_i(s)A_1(s)g_{m2,k}}{Y_o(s+jk\omega_0)} \quad k \neq 0 \end{cases} \qquad (27)$$

Next, symbolic expressions were generated for the input/output HTM elements $\tilde{H}_{0,0}(s)$, $\tilde{H}_{0,1}(s)$ and $\tilde{H}_{0,2}(s)$. These elements model the downconversion behavior of the signal contents around respectively 0, f_0 and $2f_0$ to baseband. Computations were done up to first order in the dummy variable μ (see equation (24)), while taking 7 tones into account (i.e. the HTF's $H_{-3}(s)$ to $H_3(s)$). In the absence of a priori knowledge concerning design parameter values, these settings were selected manually. In what follows, these symbolic expressions are verified numerically for a mixer with a bandwidth of 1MHz and an local oscillator frequency $f_0 = 20$MHz. Numerical computation of the HTM elements was done using an algorithm similar to the one in [10] (without the model reduction part). Comparison of the numerical results with the symbolic approximations was done by integrating the error over the interval $[0, f_0]$, with a weight function that emphasizes the characteristic in the 1MHz passband by a factor of 10dB.

The desired downconversion behavior from f_0 to baseband, determined by $\tilde{H}_{0,1}(s)$, is dominated by the contribution of 0-th order in μ. It is given by

$$\tilde{H}_{0,1}(s) = \frac{1}{2} \frac{\beta V_{osc} G_0(s)}{\left(1 - G_0(s) - \frac{H_c(s)\left(g_{m2,0}+sC_c\right)}{Y_o(s)}\right) Y_{fb}(s)} \qquad (28)$$

with V_{osc} here being the amplitude of the local oscillator signal. This expression is found to be accurate up to -81 dB.

For the HTM elements $\tilde{H}_{0,0}(s)$ and $\tilde{H}_{0,2}(s)$, things are more complicated. The expression for $\tilde{H}_{0,0}(s)$ contains 11 terms, while the one for $\tilde{H}_{0,2}(s)$ contains 8 terms, no one really dominating. As an example, we list the first couple of terms of $\tilde{H}_{0,2}(s)$,

$$\begin{aligned} \tilde{H}_{0,2}(s) \quad = \quad & \frac{1}{2} \frac{\beta V_{osc} G_{-1}(s+j\omega_0)}{L(s) Y_{fb}(s+j\omega_0)} \\ & + \frac{\beta V_{osc} G_0(s+j\omega_0) G_{-1}(s+j\omega_0)}{L(s) L(s+j\omega_0) Y_{fb}(s+j\omega_0)} \\ & - \frac{1}{2} \frac{\gamma \beta^2 V_{osc} V_{n,-1} G_0(s) H_i(s+j\omega_0)}{L(s) Y_{fb}(s) Y_{fb}(s+j\omega_0)} \\ & + \ldots \end{aligned} \qquad (29)$$

where $L(s) = 1 - G_0(s) - \frac{H_c(s)\left(g_{m2,0}+sC_c\right)}{Y_o(s)}$, the $G_k(s)$ are as defined in (27) and the $V_{n,k}$ are the Fourier coefficients corresponding to the time-varying operating point $V_n(t)$ in equation (25). For purpose of analysis, these terms can further be grouped by combining those terms having a proportional low-frequency behavior, which, in most cases, is the frequency range of interest. To do so, we use the fact that, typically, for $|s| \ll \omega_0$ and $k \neq 0$, the factors of the form $H(s + jk\omega_0)$ occurring in the terms above can be approximated as $H(s + jk\omega_0) \approx H(jk\omega_0)$, i.e. a constant. Grouping terms in this way, $\tilde{H}_{0,0}(s)$ contains 3 components and $\tilde{H}_{0,2}(s)$ 2, providing a much better starting point for analyzing and interpreting the expressions.

The accuracy of these symbolic models, as compared to direct numerical computation of the HTM elements, is listed in Table I. The results show that the expressions, generated up to first order in the dummy variable μ, allow to model $\tilde{H}_{0,0}(s)$ and $\tilde{H}_{0,2}(s)$ up

HTM element	Relative accuracy
$\tilde{H}_{0,0}(s)$	-53.8 dB
$\tilde{H}_{0,1}(s)$	- 81.0 dB
$\tilde{H}_{0,2}(s)$	-33.5 dB

Table I. Relative accuracy of the computed symbolic models as compared to direct numerical computation.

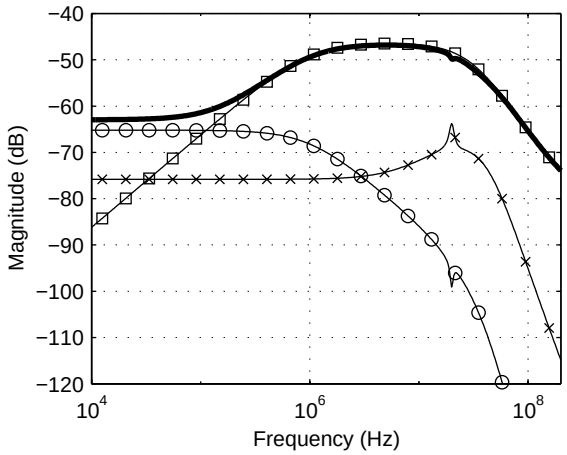

Figure 8. Exact transfer characteristic of $\tilde{H}_{0,0}(s)$ (solid bold line) and it's symbolically generated components (marked lines).

to accuracies of respectively 0.2% and 2%, with the expression for $\tilde{H}_{0,1}(s)$ being even more accurate. This is quite sufficient for most purposes. Fig. 8 and 9 plot $\tilde{H}_{0,0}(s)$ and $\tilde{H}_{0,2}(s)$ and their components for the chosen numerical setup. The solid bold line represents the exact overall transfer characterisic, while the marked lines correspond to the individual, symbolically generated components (after being grouped).

Computing contributions up to higher order in μ rapidly leads to an explosion in the number of terms and simplification techniques [2], [14] become unavoidable to control this explosion. This however requires numerical data concerning the building block parameters, which is often not available when performing symbolic computations. The results in Table I however indicate that the contribution of these higher order terms to the overall characteristic is neglegible, making it in most cases unnecessary to compute them. Up to first order, the number of terms is small enough for the generated expressions to be useful and interpretable.

6 Conclusions

This paper presented the Symbolic HTM algorithm for generation of symbolic expressions for the harmonic transfer functions of LPTV systems, starting from a behavioral model in the form of a block diagram. These expressions relate the overall input/output behavior of the LPTV system to the characteristics of its building blocks. The method is useful for deriving design equations, providing insight into the system's internal structure and for the generation of parametrised models useful for simulation and trade-off analysis at higher levels of abstraction. Symbolic HTM is based upon the organisation of the harmonic transfer functions into a harmonic transfer matrix. This allows to manipulate LPTV systems in a way that is largely similar to LTI systems, providing an efficient framework for symbolic computations. The approach was

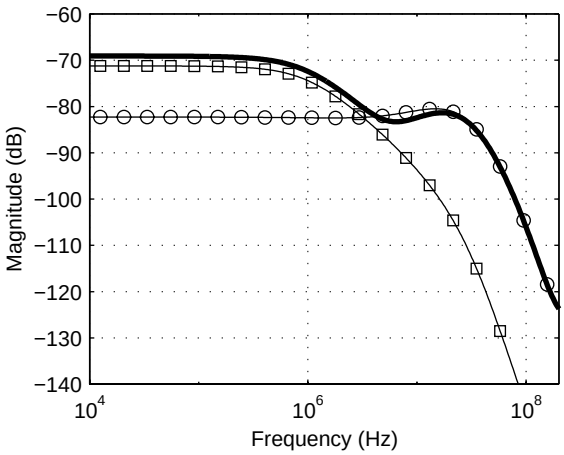

Figure 9. Exact transfer characteristic of $\tilde{H}_{0,2}(s)$ (solid bold line) and it's symbolically generated components (marked lines).

illustrated through the analysis of a downconversion mixer.

7 Acknowledgements

This work has been supported in part by the Flemish IWT.

References

[1] W. Daems, W. Verhaegen, P. Wambacq, G. Gielen and W. Sansen, "Evaluation of error-control strategies for the linear symbolic analysis of analog integrated circuits", In *IEEE Trans. Circ. and Syst.*, vol. 46, no. 5, pp. 594-606, May, 1999.

[2] F. Fernandez, A. Rodríguez-Vázquez, L. Huertas and G.Gielen, *Symbolic analysis techniques-Applications to Analog Design Automation*, IEEE Press, 1998.

[3] G. Gielen, P. Wambacq, W. Sansen, "Symbolic analysis methods and applications for analog circuits: a tutorial overview", In *Proc. of the IEEE*, vol. 82, no. 2, pp. 287-304, February, 1994

[4] G. Gielen and W. Sansen, *Symbolic Analysis for Automated Design of Analog Integrated Circuits*, Kluwer Academic Publishers, 1991

[5] G.H. Golub and C.F. Van Loan, *Matrix Computations*, 3rd edition, The John Hopkins University Press, 1996

[6] F. Leyn, W. Sansen, and G. Gielen, "Transforming Small-Signal Modeling into Control System Modeling", In *Proc. CICC*, pp. 23.1.1-4, 1998

[7] P.M. Lin, *Symbolic Network Analysis*, Elsevier, 1991

[8] E. Möllerstedt and B. Bernhardsson, "Out of Control Because of Harmonics", In *IEEE Control Systems Magazine*, pp. 70-81, 2000

[9] J. Roychowdhury, D. Long and P. Feldmann, "Cyclostationary noise analysis of large RF circuits with multitone excitations", In *IEEE Journ. Solid State Circ.*, vol. 33, no.3, pp. 324-336, March 1998

[10] J. Roychowdhury, "Reduced-order modeling of time-varying systems", In *IEEE Trans. Circ. and Syst. II*, vol. 46, no. 10, pp. 1273-1288, October 1999

[11] K. Thulasiraman and M. Swamy, *Graphs: theory and algorithms*, John Wiley & Sons Inc., 1992

[12] W. Verhaegen and G. Gielen, "Symbolic Distortion Analysis of Analog Integrated Circuits", In *Proc. ECCTD*, pp. I.21-I.24, August 2001

[13] P. Wambacq and W. Sansen, *Distortion analysis of analog integrated circuits*, Kluwer Academic Publishers, 1998

[14] P. Wambacq, G. Gielen and W. Sansen, "Symbolic network analysis methods for practical analog integrated circuits: a survey", In *IEEE Trans. Circ. and Syst.*, vol. 45, no. 10, pp. 1331-1341, October 1998.

[15] L.A. Zadeh, "Time-Varying Networks, I", In Proc. IRE, 49, pp. 1488-1503, October 1961